THE JOURNAL OF PHYSICAL CHEMISTRY A

Article

Cite This: J. Phys. Chem. A 2019, 123, 9874−9880

pubs.acs.org/JPCA

On the Impact of Singularities in the Two-State Adiabatic to Diabatic State Transformation: A Global Treatment

Yuchen Wang, Yafu Guan, and David R. Yarkony*

Department of Chemistry, Johns Hopkins University, Baltimore, Maryland 21218, United States

ABSTRACT: Diabatizations based on molecular properties can remove the singularity in the derivative coupling at a conical intersection in the diabatic representation. Yet, they can also create new singularities in the derivative couplings because of the defining equations of the adiabatic to diabatic state transformation. In the iconic two-state case, these singularities occur at points termed diabolical singular points and form a seam of dimension N^{int}-2, where N^{int} is the number of internal degrees of freedom. This seam is of the same dimension as the conical intersection seam, but is distinct. Here, the global topography of the diabolical singularity seam of 1,2^{1}A states of ammonia is reported using a Boys localization (BL) dipole-based diabatization and juxtaposed with a previously reported global representation of the coupled electronic state potential energy surfaces. The principal finding is that the seam of BL diabatization-induced singularities passes very close to the key saddle point on the 2^{1}A potential energy surface which connects the 2^{1}A equilibrium structure with the $NH_2(\tilde{X},\tilde{A})$ + H channel. The construction and detailed study of the reported diabolical singularity seam is made possible by a recently constructed analytic representation of the dipole and transition dipole moment surfaces.

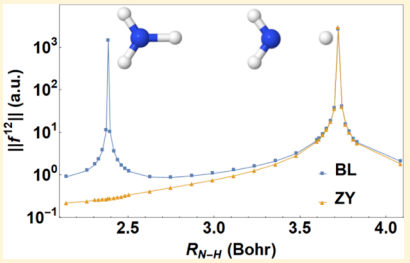

1. INTRODUCTION

The adiabatic to diabatic (AtD) states transformation **U** is an $N^{state} \times N^{state}$ unitary transformation, mapping the well-defined adiabatic states, solutions of the electronic Schrödinger equation, to single-valued diabatic states, states for which the residual derivative coupling is reduced significantly.[1−3] There are many approaches to construction of a quasi-diabatic representation, including configuration uniformity,[4−6] molecular properties,[7,8] localized charges,[9,10] least-squares minimization of the residual couplings,[11] ansatz,[12,13] and line integrals.[14−16]

Two-state diabatizations are of particular interest because in addition to their use in describing two-state nonadiabatic dynamics, the derivative coupling deduced from the AtD transformation for states I and I + 1 can be used to construct the vector potential needed to quantify the effect of the geometric phase induced by energetically inaccessible conical intersections of states I and I + 1 on single-state (adiabatic state I) dynamics.[17−19]

In a previous paper,[20] Zhu and Yarkony turned to an issue in property-based diabatizations termed diabolical singularities, singularities in the derivative coupling unrelated to conical intersections. A method to locate these diabolical singular points (DSPs), by minimizing a Lagrangian was proposed. The method, formally similar to the procedure used to locate conical intersections,[21] was subsequently implemented and applied to the 1,2^{1}A states of methylamine,[22] where it was shown that the Boys localization (BL) diabatization,[10] a property-based diabatization described below, will produce infinite derivative couplings in energetically accessible regions of nuclear coordinate space where the two adiabatic states are well separated. The procedure, however, uses derivatives of dipole moments, which are costly to evaluate even with modern electronic structure theory.

Previously, Zhu and Yarkony have introduced a diabatization scheme (here denoted the ZY diabatization) which simultaneously fits and diabatizes ab initio electronic structure data, by minimizing, in a least-squares sense, the difference between the ab initio and fit energies, energy gradients, and the energy difference scaled derivative coupling.[23] The inclusion of the energy difference scaled derivative coupling in the fit precludes DSPs in the ZY method. The fitted surfaces have been used in multiple quantum dynamic simulations and produce convincing results.[24,25] More recently, Guan et al. have reported a neural network extension of the ZY diabatization.[26,27]

The matrix elements of molecular properties operators $(O^{(k)}(\mathbf{r};\mathbf{q}))$ in the adiabatic/diabatic representation, $\Psi_J^{(x)}(\mathbf{r};\mathbf{q})$, become surfaces $O_{I,J}^{(x)(k)}(\mathbf{q})$ where

$$O_{I,J}^{(x)(k)}(\mathbf{q}) = \langle \Psi_I^{(x)}(\mathbf{r};\mathbf{q}) | O^{(k)}(\mathbf{r};\mathbf{q}) | \Psi_J^{(x)}(\mathbf{r};\mathbf{q}) \rangle_{\mathbf{r}} \quad (1)$$

Here, (x) = (a) for adiabatic and (d) for diabatic, **r** denotes the electronic coordinates, and **q** denotes the 3 N^{atom}-6 internal nuclear coordinates. The diabatic, but not the adiabatic, property surfaces are smooth, allowing them also to be fit analytically.

This work explicitly considers ammonia photodissociation

$$NH_3(1^1A) + h\nu \rightarrow NH_3(2^1A) \rightarrow NH_2(1, 2^2A) + H \quad (2)$$

Received: September 7, 2019
Revised: October 12, 2019
Published: October 16, 2019

DOI: 10.1021/acs.jpca.9b08519
J. Phys. Chem. A 2019, 123, 9874−9880

The computational focus will be on the frequently used BL diabatization as described by Subotnik and Ratner.[10,28] The analysis is, however, generally applicable to any property operator, for which the AtD transformation angle $\Theta(\mathbf{q})$ is given by

$$\tan m\Theta(\mathbf{q}) = n(\mathbf{q})/d(\mathbf{q}) \tag{3}$$

Previously,[20] a diabolical singularity was demonstrated, at a single point on its seam, for the above system using the dipole-based diabatization of Werner and Meyer.[7] Here, $m = 2$ for single operator diabatization and $m = 4$ for the BL diabatization.[20] As described in Section 1, $n(\mathbf{q})$ and $d(\mathbf{q})$ in the BL diabatization are smooth functions of the dipole and transition dipole matrix elements. For the 1^1A and 2^1A states of ammonia diabatic dipole moment and transition dipole moment surfaces (DMSs) for $O^{(k)} = \mu^{(k)}$, $k = (x, y, z)$ have been fitted with neural networks exploiting the accurate ZY quasi-diabatic representation reported previously.[29−31] These DMSs are very accurate in the sense that the ab initio dipole and transition dipole moments are well reproduced in the relevant regions. Through these DMSs, the derivatives of the dipole and transition dipole moments required to locate DSPs can be obtained numerically by divided differences, the computational cost of which is negligible compared to divided differences based on ab initio calculations. The new fitting method which can be readily extended to other properties enables the global analysis of the seam of diabolical singularities reported herein.

Section 2 reviews the two types of singularities of the adiabatic state derivative couplings considered in this work. Section 3 discusses the space of diabolical singularities for the BL diabatization relevant to the ammonia photodissociation in 2; the summary and conclusion are given in Section 4.

2. THEORETICAL APPROACH

We are concerned with the commonly used two-state adiabatic ($\Psi_I^{(a)}(\mathbf{r};\mathbf{q})$) to diabatic ($\Psi_\alpha^{(d)}(\mathbf{r};\mathbf{q})$) state (AtD) transformation of the form.

$$\begin{pmatrix}\Psi_\alpha^{(d)}(\mathbf{r};\,\mathbf{q})\\ \Psi_\beta^{(d)}(\mathbf{r};\,\mathbf{q})\end{pmatrix} = \begin{pmatrix}\cos\Theta(\mathbf{q}) & -\sin\Theta(\mathbf{q})\\ \sin\Theta(\mathbf{q}) & \cos\Theta(\mathbf{q})\end{pmatrix}\begin{pmatrix}\Psi_I^{(a)}(\mathbf{r};\,\mathbf{q})\\ \Psi_J^{(a)}(\mathbf{r};\,\mathbf{q})\end{pmatrix} \tag{4}$$

The derivative coupling in the adiabatic basis is given by

$$\begin{aligned}\mathbf{f}^{J,I,(a)}(\mathbf{q}) &= \langle\Psi_J^{(a)}(\mathbf{r};\,\mathbf{q})|\nabla_{\mathrm{q}}\Psi_I^{(a)}(\mathbf{r};\,\mathbf{q})\rangle_{\mathbf{r}}\\ &= \nabla_{\mathrm{q}}\Theta(\mathbf{q}) + \mathbf{f}^{\beta,\alpha,(d)}(\mathbf{q})\end{aligned} \tag{5}$$

where $\nabla_q^\dagger = \left(\frac{\partial}{\partial q_1}, \ldots, \frac{\partial}{\partial q_{N^{\mathrm{int}}}}\right)$ and $\mathbf{f}^{\beta,\alpha,(d)}(\mathbf{q})$, the derivative coupling in the diabatic basis is usually small and can be ignored. The rotation angle Θ in a property-based diabatization is determined from an expression of the form of eq 3, where $n(\mathbf{q})$ and $d(\mathbf{q})$ are smooth functions of the $O_{I,J}^{(a),w}(\mathbf{q})$.

It was shown that using eqs 1, 3−5, the property-based diabatizations will be able to remove the singular part of the derivative coupling arising from a conical intersection and construct a diabatic representation.[32,33] However, this treatment creates a new problem.[20,34] The rotation angle defined by eq 3 has an N^{int}-2 dimensional seam of singularities where

$$n(\mathbf{q}) = 0, \qquad d(\mathbf{q}) = 0 \tag{6}$$

As illustrated in ref 20, the adiabatic derivative couplings obtained at these points using eq 5 are infinite. These singular points are referred to as DSPs.[20] The situation is illustrated in Figure 1 which plots the magnitude of the derivative coupling

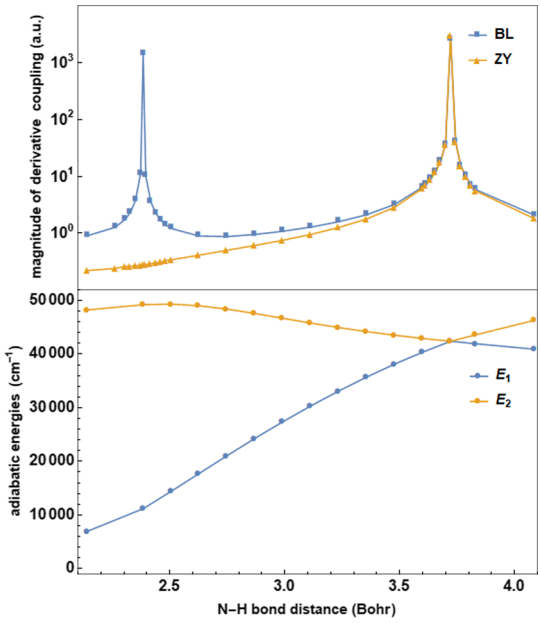

Figure 1. Derivative couplings obtained from BL and ZY diabatization (upper panel) and the adiabatic energies (lower panel) along a linear synchronous transit path connecting the minimum E_2 energy DSP and the MEX.

obtained from the BL and the ZY diabatizations, along an extended linear synchronous transit path connecting the two types of singularities considered in this work. For the BL diabatization, $\mathbf{O} = (\mu_x, \mu_y, \mu_z)$ denotes the three distinct dipole operator components, and the numerator and denominator in eq 3 take the following form[10,20]

$$\begin{aligned}n(\mathbf{q}) &= 4(\mathbf{O}_{1,1}^{(a)} - \mathbf{O}_{2,2}^{(a)})\cdot\mathbf{O}_{1,2}^{(a)}\\ d(\mathbf{q}) &= |(\mathbf{O}_{1,1}^{(a)} - \mathbf{O}_{2,2}^{(a)})|^2 - 4|\mathbf{O}_{1,2}^{(a)}|^2\end{aligned} \tag{7}$$

Because the BL diabatization involves all three dipole moment components, it might be hoped that this would limit the geometries for which both $n(\mathbf{q})$ and $d(\mathbf{q})$ vanish, but this turns out not to be the case.

Equation 6 defines the entire N-2 dimensional degeneracy space. To define a single unique point on this seam, we require energy minimization of either state I or J. Additional points on the seam are obtained by imposing geometrical constraints $K_i(\mathbf{q}) = 0$, $i = 1, \ldots, N^{\mathrm{c}}$. Thus, we need to find $\mathbf{q}$ which optimizes E_{P}, $P = I$ or J subject to the geometric constraints and the requirement/constraint that $\mathbf{q}$ be a DSP. This is accomplished using a Lagrange multiplier constrained optimization with the following Lagrangian

$$\begin{aligned}&L_{\mathrm{P}}(\mathbf{q}, \lambda_1, \lambda_2, \kappa_1, \ldots\kappa_{N^{\mathrm{c}}})\\ &\quad = E_{\mathrm{P}}(\mathbf{q}) + \lambda_1 n(\mathbf{q}) + \lambda_2 d(\mathbf{q}) + \sum_{i=1}^{N^{\mathrm{c}}}\kappa_i K_i(\mathbf{q})\end{aligned} \tag{8a}$$

where λ_s, and κ_i are Lagrange multipliers. This gives a system of linear equations

DOI: 10.1021/acs.jpca.9b08519
J. Phys. Chem. A 2019, 123, 9874−9880

Table 1. DSP Obtained from Ab Initio and Fit Dipole Surface[a]

	numerator	denominator	$R(NH_1)$	$R(NH_3)$	$\angle H_1NH_2$	E_1	E_2
DSP (ab initio)	1.81×10^{-8}	-2.75×10^{-5}	1.2622	1.0380	123.11	11 191	49 238
DSP (fit)	3.62×10^{-6}	-2.72×10^{-6}	1.2616	1.0381	123.00	11 175	49 227

[a]Distances in Å, angles in degree, energy in cm^{-1}.

$$\begin{pmatrix} \frac{\partial^2 L_P}{\partial \mathbf{q}\partial \mathbf{q}} & (\nabla n, \nabla d) & (\nabla \mathbf{K}) \\ (\nabla n)^\dagger & 0\ \ 0 & \\ (\nabla d)^\dagger & 0\ \ 0 & 0 \\ (\nabla \mathbf{K})^\dagger & 0 & 0 \end{pmatrix} \begin{pmatrix} \delta q \\ \delta\lambda_1 \\ \delta\lambda_2 \\ \delta\kappa \end{pmatrix} = -\begin{pmatrix} \nabla L_P \\ n \\ d \\ \mathbf{K} \end{pmatrix} \tag{8b}$$

The use of eq 8b to determine the seam of singularities has been discussed previously[22] based on the use of ab initio dipoles and transition dipoles and their numerical divided difference derivatives. The use of ab initio data is numerically cumbersome and limits the portion of the seam that can be practically obtained.

3. RESULTS AND DISCUSSION

Section 2 discussed the possible insidious effects diabolical singularities associated with a two-state property-based diabatization can have on the derivative couplings which are at the heart of nonadiabatic dynamics. In this section, we consider whether diabolical singularities obtained using a standard diabatization technique, the BL diabatization, have sufficient support that they could affect the outcome of nonadiabatic photodissociation in a realistic system.

Table 2. Number of Points with a Small Numerator and Denominator in the 3003-Point Set

$n^2 + d^2$ threshold	number of points
0.01	833
0.001	342
0.0001	53
0.00001	10

3.1. Fit Representations. In this work, we consider reaction 2 ammonia photodissociation from its first excited state. The original ab initio description is based on a previously reported multireference single and double excitation configuration interaction calculation of the electronic structure data,[29] including energies, energy gradients, and derivative couplings, to which we recently added dipoles and transition dipoles. For more detail concerning the electronic structure method used, see ref 29. All energies reported here are relative to the ground-state minimum $E_0 = -56.47598618$ hartree. The ZY diabatization scheme, noted above, used the energies, energy gradients, and derivative couplings to construct a coupled diabatic state representation $\mathbf{H}^d$ of this system.[29] The dipoles and transition dipoles were represented by recently constructed, compatible, analytic representations based on neural networks constructed from data at 3003 points.[27] Combining the two fits allows us to perform a global analysis of the diabolical singularities based on high quality electronic structure data.

Table 3. Derivative couplings of five Random Points Picked from the $|n^2 + d^2| < 0.1^2$ Data Set

	numerator	denominator	$\lvert f_{12}\rvert$ (BL) (au)	$\lvert f_{12}\rvert$ (ZY) (au)	$\lvert f_{12}\rvert$ (ab initio) (au)
1	−0.02994948	−0.05743443	2.55	0.55	0.58
2	−0.03630134	−0.04356971	4.71	0.39	0.48
3	0.05973111	−0.02849410	1.17	1.17	1.09
4	0.01967043	−0.00406466	10.74	1.28	1.29
5	0.02340189	−0.01295294	0.64	0.51	0.60

The $\mathbf{H}^d$ and dipole fits provide the "ab initio" data in a fraction of the time required for true ab initio calculations. Given the reported root mean square errors, the fit dipole and coupled energy surfaces are expected to provide accurate representations of the ab initio data. To test this assumption, we compare the structure and E_2 energy of the minimum energy DSP computed fully ab initio and computed entirely from the fit surfaces. Table 1 below compares the geometries and energetics at this point. The good agreement between fit and ab initio result is not unexpected.

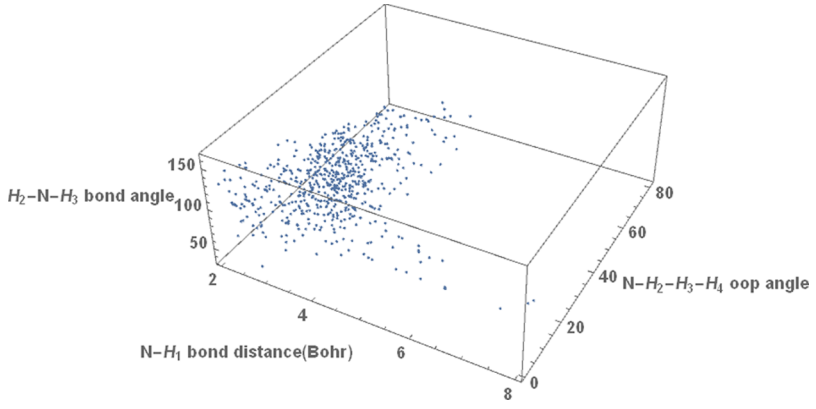

Figure 2. Ab initio points with $|n^2 + d^2| < 0.01$ expanded in three-internal-coordinate space. The out-of-plane angle is defined as $\phi = \arcsin[\mathbf{e}_{N,H_1} \cdot (\mathbf{e}_{H_1,H_2} \times \mathbf{e}_{H_1,H_3})/|\mathbf{e}_{H_1,H_2} \times \mathbf{e}_{H_1,H_3}|]$.

DOI: 10.1021/acs.jpca.9b08519
J. Phys. Chem. A 2019, 123, 9874−9880

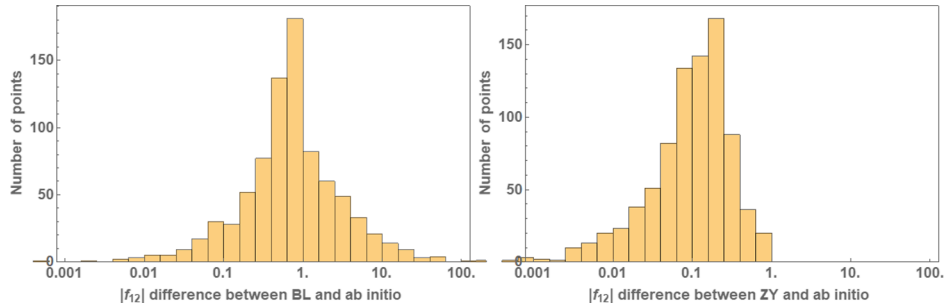

Figure 3. Differences in derivative couplings (compared to ab initio values) for BL (left) and ZY (right) diabatization respectively. Data points are taken to be the 833 points with $|n^2 + d^2| < 0.01$.

Table 4. Key Parameter during a Single DSP Search Process

	numerator	denominator	E_1 (cm^{-1})	E_2 (cm^{-1})	$\|f_{12}\|$ (BL) (au)	$\|f_{12}\|$ (ZY) (au)	$\|f_{12}\|$ (ab initio) (au)
0	-2.70×10^{-2}	1.71×10^{-2}	13 632.61	49 327.96	1.5	0.26	0.27
1	5.97×10^{-3}	9.78×10^{-2}	11 855.61	49 330.52	0.8	0.29	0.31
2	2.19×10^{-3}	-1.72×10^{-3}	11 167.80	49 228.43	109.6	0.27	0.28
3	2.75×10^{-6}	2.08×10^{-4}	11 171.09	49 228.19	425.2	0.27	0.28
4	-9.52×10^{-8}	2.13×10^{-5}	11 174.22	49 227.46	674.4	0.28	0.28

Table 5. Geometry and Energy of critical Points on the Excited State[a]

	$R(NH_1)$	$R(NH_2)$	$R(NH_3)$	$\angle H_1NH_2$	$\angle H_1NH_3$	E_1	E_2
min2D3h	1.0485	1.0485	1.0485	120.00	120.00	3266	47 171
sad2C2v	1.3054	1.0408	1.0408	123.77	123.77	13 635	49 347
mexC2v	1.9689	1.0222	1.0222	125.46	125.46	42 400	42 400
DSP(minE2)	1.2616	1.0381	1.0381	123.00	123.00	11 175	49 227

[a]Out of plane angle $\phi = 0$, distances in Å, angles in degree, energy in cm^{-1}.

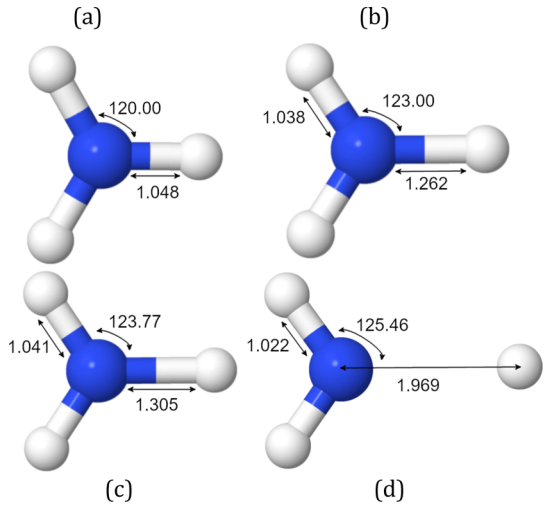

Figure 4. Important geometries (a) 2^1A state D_{3h} minimum and (b) minimum E_2 energy DSP. (c) 2^1A saddle point and (d) minimum energy 1^1A-2^1A conical intersection.

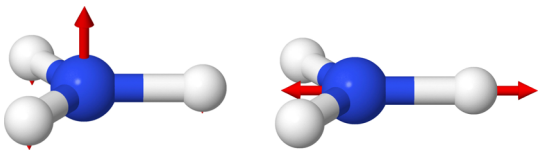

Figure 5. Gradient of numerator (left) and denominator (right) at E2min DSP after normalization in terms of atom centered vectors.

3.2. Constructing the DSP Seam. The dipole and transition dipole fits will enable us to obtain the derivative couplings from the BL diabatization using eq 4 and dipole derivatives without additional ab initio calculations. This greatly facilitates the mapping and interpreting of the DSP seam. Divided difference of fit dipole data rather of ab initio dipole data itself accelerates the optimization process based on eq 8b and allows for a more comprehensive study of the diabolical singularity seam. Moreover, in eq 8b, in the original ab initio treatment, we approximated the hessian of Lagrangian with a diagonal matrix.[22] This treatment, although reducing the computational cost significantly while still being effective, limited the optimization accuracy. Again, by using the fitted dipole surface, the full second derivative of dipole moment can be calculated numerically, which allows us to compute the hessian of the Lagrangian without approximation.

To determine the extent of the DSP seam and to see whether the diabolical singularities occur in a dynamically relevant region, we first search for points with a small numerator and denominator in the ab initio data set used to construct the dipole fit. The results are listed in Table 2; 833 points, 27.7% of the total points satisfy the condition $|n^2 + d^2| < 0.01$. A detailed figure (Figure 2) is made by plotting the 833 points along three internal coordinates (the longest N−H distance, denoted $N-H_1$, the bond angle of H_2-N-H_3 and the out-of-plane angle $N-H_1-H_2-H_3$). From Figure 2, we conclude that the points are distributed over a wide range of nuclear coordinates. As these points are originally generated from quasi-classical trajectories,[29] we believe that small numerator and denominator points are frequently encountered

DOI: 10.1021/acs.jpca.9b08519
J. Phys. Chem. A 2019, 123, 9874−9880

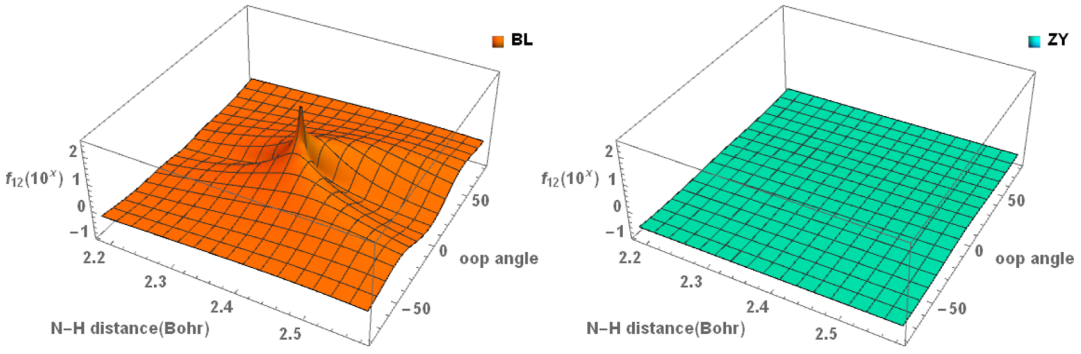

Figure 6. Plate (a) f_{12} near the minimum energy DSP expanded in N–H distance and H–N–H–H out-of-plane directions. (b) Same as Plate (a) except ZY diabatization data used.

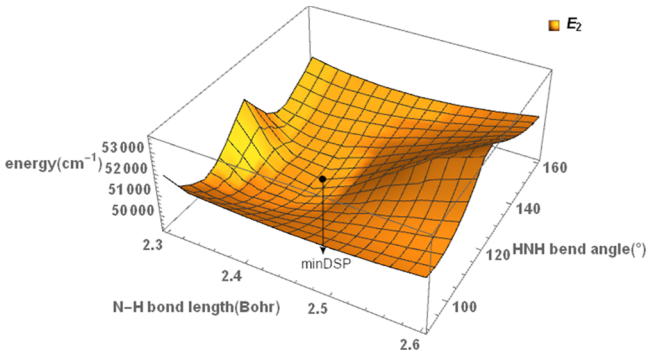

Figure 7. DSPs on the 2-D grid of the diabolical singularity seam spanned by the N–H bond distance and HNH bond angle. At minDSP = E2min E_1(E2min) = 11 175 cm^{-1}, E_2(E2min) = 49 227 cm^{-1} from the fit.

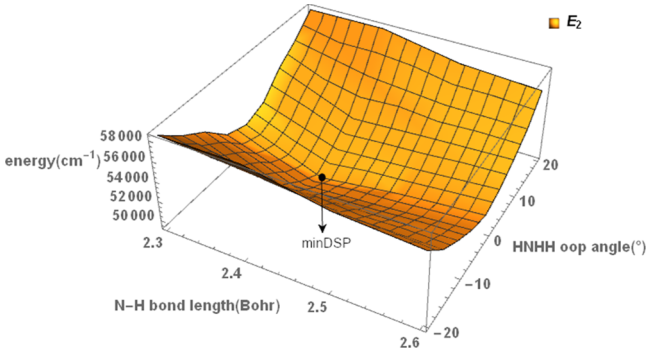

Figure 8. DSPs on the 2-D grid of the diabolical singularity seam spanned by the N–H bond distance and HNHH out-of-plane bond angle. At minDSP = E2min E_1(E2min) = 11 175 cm^{-1}, E_2(E2min) = 49 227 cm^{-1} from fit.

during dynamic simulations, which means that the DSP seam will significantly affect the dynamics of photodissociation.

Because the BL derivative couplings of these points can be obtained from the fit dipole and transition dipole surfaces using eq 4, it is important to compare them with the ab initio- and ZY diabatization-determined values. This will give us a preliminary impression about when the BL values are no longer valid. We pick five random points with $|n^2 + d^2| < 0.01$ from the 833 point data set above for test purposes. The BL and ZY diabatization determined derivative couplings are compared with the corresponding ab initio determined

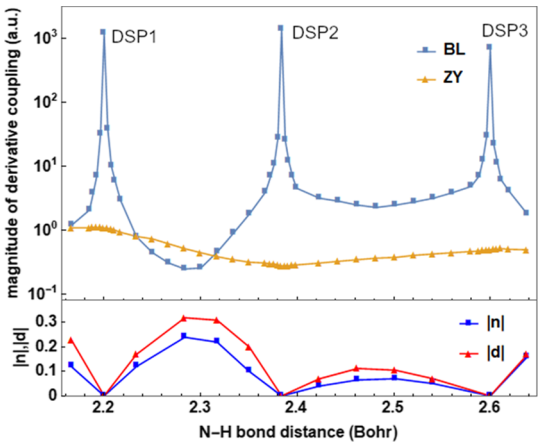

Figure 9. Derivative couplings from BL and ZY (upper panel) and |*n*|, |*d*| (lower panel) along a linear synchronous transit path passing three different DSPs. Ab initio energy E_2 (E_1) of three DSPs are presented, E(DSP1) = 51 686(10 623) cm^{-1}, E(DSP2) = 49 234(11 167) cm^{-1}, E(DSP3) = 51 501(32 913), excited state energy first and ground state in parentheses.

quantities in Table 3. While the ZY diabatization and ab initio-determined derivative couplings are in good agreement, with the exception of point 3 and 5, such good agreement between BL diabatization and ab initio determined quantities is not found.

Figure 3 provides an alternative perspective taking the difference between BL diabatization and ab initio determined derivative coupling for the 833 points above. For comparison, the difference between the ZY- and ab initio-determined quantities is also plotted. While for some points, the agreement between BL and ab initio is satisfactory, the remainder do not agree very well. These points are not on the N^{int}-2 seam exactly, but rather in the vicinity of the seam. The derivative couplings produced by BL diabatization in those regions are far from infinity, but still unreliable.

Using a point from the initial scan (Figure 2) as a starting guess, we then seek energy-minimized DSPs ($n \approx 0$, $d \approx 0$) on the excited-state surface by optimizing the Lagrangian in eq 8a. Our search begins at one random point in the above data set with both numerator and denominator at ~0.01 in magnitude. The search locates the desired minimum energy DSP within five iterations. A detailed analysis of the search iterations, including the derivative coupling from three sources, BL, ZY

DOI: 10.1021/acs.jpca.9b08519
J. Phys. Chem. A 2019, 123, 9874–9880

diabatizations, and ab initio, is provided in Table 4. The derivative coupling from ZY diabatization differs little from the ab initio result, which agrees with our previous discussion of the fit accuracy.[29] The derivative coupling from BL diabatization, however, is abnormally large, while the ab initio result is small, and the two states are well separated. The fallacious derivative coupling increases to over 100 a.u. when the numerator and denominator become small enough. Errors of this size could have an impact on nonadiabatic transition.

For reference, the geometry of the excited-state energy of minimum, saddle point, minimum energy conical intersection, and minimum energy DSP(minE2) are listed in Table 5 and shown in Figure 4. Note that all points here have C_{2v} symmetry, which is a consequence of the energy minimization conditions. The energy of the DSP, minE2, is lower than the saddle point by 120 cm^{-1}, and both points are in the same geometric region. Given the fact that the saddle point region is accessible during the dissociation, the system should also have enough energy to access the DSPs or their neighborhood.

The gradient of $n(\mathbf{q})$ and $d(\mathbf{q})$, which lift the degeneracy of the diabolical seam linearly, is shown in Figure 5. It is not surprising that ∇n is the out of plane motion as the numerator here vanishes by symmetry.

Figure 6 describes the topography of the derivative coupling in the vicinity of a DSP (here E2min). From E2min, we expand the space in the N−H stretch and H−N−H−H out-of-plane directions, which are also the main component of ∇n and ∇d. The BL diabatization derivative coupling is singular at the origin, while the ZY diabatization-derived coupling is small. We also observed that for points in the vicinity of the seam, especially points on the ridge, the BL diabatization-deduced derivative coupling is still larger than the ZY diabatization-deduced values, but far from singular. Those points are deleterious and yet hard to detect.

To understand the global topography of the seam, Figures 7 and 8 describe the DSP seam as a function of two internal coordinates starting from E2min. To do this, we include geometric constraints $K(\mathbf{q})$: $q_i = x$, $q_j = y$ in the Lagrangian in eq 8a. This is done on uniform grids (choice of x, y) $K(\mathbf{q})$: $q_i = x$, $q_j = y$. Figures 7 and 8 present the results for two grids: NH bond distance (spacing 0.02 bohr) with H−N−H bond angle (spacing 2.5°) and NH bond distance (spacing 0.05 bohr) with out-of-plane angle (spacing 5°). Each point on the surface is an optimized energy-minimized point with two geometry constraints. In Figure 7, with the unconstrained out-of-plane angle, the optimization always ends up with the out-of-plane angle close or equal to 0. As mentioned previously, this is due to the nature of our energy minimization condition. The symmetry, which serves as a sufficient but not necessary condition for the numerator to vanish, is broken artificially by setting one geometric constraint to the out-of-plane angle in Figure 8. As points with energy greater than 50 000 cm^{-1} were given reduced weight in the potential energy surface fitting procedure,[35] we expect slightly larger error of the energies in Figures 7 and 8. Because equal weights were used for each point in the dipole moment fit and the ab initio dipole moments have been well reproduced, we ensure that the DSPs are well optimized and some error in energies is not an major issue for plotting purpose here. For both figures, the highest energy is less than 58 000 cm^{-1}, which indicates that the diabolical singularity needs to be taken care of in a relatively large nuclear coordinate space.

Figure 9 examines the space between the seam points in Figure 7. It presents a linear synchronous transit path (not necessarily composed of seam points) connecting three distinct DSPs on the seam. For points on this arbitrary path, the size of the errors in the BL diabatization-determined derivative coupling depends largely on how "far" the numerator and denominator are from zero, in other words, how far the points are from the seam of DSPs. The failure of the BL diabatization happens not only exactly on the N^{int}-2 dimensional seam, where its occurrence is obvious, but also in the vicinity of such points where its impact on the derivative coupling is significant but perhaps not obvious, unless the correct derivative coupling is available, as shown in Figure 9. Its importance, however, could be estimated approximately from the ratio of the numerator and denominator. Thus, for nonadiabatic dynamics employing a BL diabatization, the reliability of the derivative coupling should be assessed prior to running nonadiabatic dynamics simulations.

4. CONCLUSIONS

For two-state diabatizations based on eq 3, the diabatization angle is undefined on a seam of dimension N^{int}-2 in nuclear coordinate space. This seam is mapped for the first time for the $1,2^1A$ states of NH_3 based on a standard BL diabatization. At these seam points, the adiabatic derivative couplings are infinite. These points are termed DSPs. The E_2 energy-minimized DSP lies very close to the key saddle point on the 2^1A potential energy surface. This saddle point connects the $NH_3(2^1A)$ equilibrium structure with the NH_2 + H dissociation channel. In future work, we will use nonadiabatic dynamics to quantify the effect of these singularities. The numerical calculations carried out here are made possible by the construction of analytic representations of the dipole and transition dipole surfaces.

AUTHOR INFORMATION

Corresponding Author

*E-mail: cyarkony@jhu.edu.

ORCID

David R. Yarkony: 0000-0002-5446-1350

Notes

The authors declare no competing financial interest.

ACKNOWLEDGMENTS

This work is supported by National Science Foundation grant CHE 1663692 to D.R.Y. The authors acknowledge generous grant of computer time from the Maryland Advanced Research Computing Center (MARCC) and from National Energy Research Scientific Computing Center (NERSC).

REFERENCES

(1) Mead, C. A.; Truhlar, D. G. Conditions for the Definition of a Strictly Diabatic Electronic Basis for Molecular Systems. *J. Chem. Phys.* **1982**, *77*, 6090−6098.

(2) Baer, M. Adiabatic and Diabatic Representations for Atom-Molecule Collisions: Treatment of the Collinear Arrangement. *Chem. Phys. Lett.* **1975**, *35*, 112.

(3) Baer, M. *Beyond Born Oppenheimer: Electronic Nonadiabatic CouplingTerms and Conical Intersections*. Wiley: Hoboken, New Jersey, 2006.

(4) Atchity, G. J.; Ruedenberg, K. Determination of Diabatic States through Enforcement of Configurational Uniformity. *Theor. Chem. Acc.* **1997**, *97*, 47−58.

DOI: 10.1021/acs.jpca.9b08519
J. Phys. Chem. A 2019, 123, 9874−9880

(5) Yang, K. R.; Xu, X.; Truhlar, D. G. Direct Diabatization of Electronic States by the Fourfold-Way: Including Dynamical Correlation by Multi-Configuration Quasidegenerate Perturbation Theory with Complete Active Space Self-Consistent-Field Diabatic Molecular Orbitals. *Chem. Phys. Lett.* **2013**, *573*, 84−89.
(6) Xu, X.; Yang, K. R.; Truhlar, D. G. Diabatic Molecular Orbitals, Potential Energies, and Potential Energy Surface Couplings by the 4-Fold Way for Photodissociation of Phenol. *J. Chem. Theory Comput.* **2013**, *9*, 3612−3625.
(7) Werner, H.-J.; Meyer, W. Mcscf Study of the Avoided Curve Crossing of the Two Lowest $^1\sigma^+$ States of Lif. *J. Chem. Phys.* **1981**, *74*, 5802−5807.
(8) Cave, R. J.; Newton, M. D. Generalization of the Mulliken-Hush Treatment for the Calculation of Electron Transfer Matrix Elements. *Chem. Phys. Lett.* **1996**, *249*, 15−19.
(9) Fatehi, S.; Alguire, E.; Subotnik, J. E. Derivative Couplings and Analytic Gradients for Diabatic States, with an Implementation for Boys-Localized Configuration-Interaction Singles. *J. Chem. Phys.* **2013**, *139*, 124112.
(10) Subotnik, J. E.; Yeganeh, S.; Cave, R. J.; Ratner, M. A. Constructing Diabatic States from Adiabatic States: Extending Generalized Mulliken−Hush to Multiple Charge Centers with Boys Localization. *J. Chem. Phys.* **2008**, *129*, 244101.
(11) Evenhuis, C. R.; Lin, X.; Zhang, D. H.; Yarkony, D.; Collins, M. A. Interpolation of Diabatic Potential-Energy Surfaces: Quantum Dynamics on Ab Initio Surfaces. *J. Chem. Phys.* **2005**, *123*, 134110.
(12) Viel, A.; Eisfeld, W. Effects of Higher Order Jahn-Teller Coupling on the Nuclear Dynamics. *J. Chem. Phys.* **2004**, *120*, 4603−4613.
(13) Eisfeld, W.; Viel, A. Higher Order (a+E)⊗E Pseudo-Jahn−Teller Coupling. *J. Chem. Phys.* **2005**, *122*, 204317.
(14) Baer, M.; Lin, S. H.; Alijah, A.; Adhikari, S.; Billing, G. D. Extended approximated Born-Oppenheimer equation. I. Theory. *Phys. Rev. A* **2000**, *62*, 03250.
(15) Ghosh, S.; Mukherjee, S.; Mukherjee, B.; Mandal, S.; Sharma, R.; Chaudhury, P.; Adhikari, S. Beyond Born-Oppenheimer Theory for Ab Initio Constructed Diabatic Potential Energy Surfaces of Singlet H 3+ to Study Reaction Dynamics Using Coupled 3d Time-Dependent Wave-Packet Approach. *J. Chem. Phys.* **2017**, *147*, 074105.
(16) Mukherjee, B.; Mukherjee, S.; Sardar, S.; Shamasundar, K. R.; Adhikari, S. A Beyond Born-Oppenheimer Treatment of Five State Molecular System No3 and the Photodetachment Spectra of Its Anion. *Chem. Phys.* **2018**, *515*, 350−359.
(17) Malbon, C. L.; Zhu, X.; Guo, H.; Yarkony, D. R. On the Incorporation of the Geometric Phase in General Single Potential Energy Surface Dynamics: A Removable Approximation to Ab Initio Data. *J. Chem. Phys.* **2016**, *145*, 234111.
(18) Xie, C.; Malbon, C. L.; Yarkony, D. R.; Xie, D.; Guo, H. Signatures of a Conical Intersection in Adiabatic Dissociation on the Ground Electronic State. *J. Am. Chem. Soc.* **2018**, *140*, 1986−1989.
(19) Xie, C.; Malbon, C. L.; Guo, H.; Yarkony, D. R. Up to a Sign. The Insidious Effects of Energetically Inaccessible Conical Intersections on Unimolecular Reactions. *Acc. Chem. Res.* **2019**, *52*, 501−509.
(20) Zhu, X.; Yarkony, D. R. On the Construction of Property Based Diabatizations: Diabolical Singular Points. *J. Phys. Chem. A* **2015**, *119*, 12383−12391.
(21) Manaa, M. R.; Yarkony, D. R. On the Intersection of Two Potential Energy Surfaces of the Same Symmetry. Systematic Characterization Using a Lagrange Multiplier Constrained Procedure. *J. Chem. Phys.* **1993**, *99*, 5251−5256.
(22) Wang, Y.; Yarkony, D. R. Determining Whether Diabolical Singularities Limit the Accuracy of Molecular Property Based Diabatic Representations: The 1,21A States of Methylamine. *J. Chem. Phys.* **2018**, *149*, 154108.
(23) Zhu, X.; Yarkony, D. R. On the Elimination of the Electronic Structure Bottleneck in on the Fly Nonadiabatic Dynamics for Small to Moderate Sized (10-15 Atom) Molecules Using Fit Diabatic Representations Based Solely on Ab Initio Electronic Structure Data: The Photodissociation of Phenol. *J. Chem. Phys.* **2016**, *144*, 024105.
(24) Xie, C.; Ma, J.; Zhu, X.; Yarkony, D. R.; Xie, D.; Guo, H. Nonadiabatic Tunneling in Photodissociation of Phenol. *J. Am. Chem. Soc.* **2016**, *138*, 7828−7831.
(25) Xie, C.; Malbon, C. L.; Xie, D.; Yarkony, D. R.; Guo, H. Nonadiabatic Dynamics in Photodissociation of Hydroxymethyl in the $3^2a(3p_x)$ Rydberg State: A Nine-Dimensional Quantum Study. *J. Phys. Chem. A* **2019**, *123*, 1937−1944.
(26) Guan, Y.; Zhang, D. H.; Guo, H.; Yarkony, D. R. Representation of Coupled Adiabatic Potential Energy Surfaces Using Neural Network Based Quasi-Diabatic Hamiltonians: 1,2 $^2a'$ States of Lifh. *Phys. Chem. Chem. Phys.* **2019**, *21*, 14205−14213.
(27) Guan, Y.; Guo, H.; Yarkony, D. R. Neural Network Based Quasi-Diabatic Hamiltonians with Symmetry Adaptation and a Correct Description of Conical Intersections. *J. Chem. Phys.* **2019**, *150*, 214101.
(28) Ou, Q.; Subotnik, J. E. Electronic Relaxation in Benzaldehyde Evaluated Via TD-DFT and Localized Diabatization: Intersystem Crossings, Conical Intersections, and Phosphorescence. *J. Phys. Chem. C* **2013**, *117*, 19839−19849.
(29) Zhu, X.; Yarkony, D. R. Toward Eliminating the Electronic Structure Bottleneck in Nonadiabatic Dynamics on the Fly: An Algorithm to Fit Nonlocal, Quasidiabatic, Coupled Electronic State Hamiltonians Based on Ab Initio Electronic Structure Data. *J. Chem. Phys.* **2010**, *132*, 104101.
(30) Guan, Y.; Guo, H.; Yarkony, D. R. Extending the Representation of Multistate Coupled Potential Energy Surfaces to Include Properties Operators Using Neural Networks: Application to the 1,2^{1}A States of Ammonia. *J. Chem. Theory Comput.* **2019**, submitted for publication.
(31) Zhu, X. GitHub-virtualzx-nad/NH_3-X-A-Coupled-PES: Global full dimensional quasidiabatic Hamiltonian for the first two singlet states of NH_3. https://github.com/virtualzx-nad/NH3-X-A-Coupled-PES (accessed Sep 1, 2019).
(32) Yarkony, D. R. Energies and Derivative Couplings in the Vicinity of a Conical Intersection Using Degenerate Perturbation Theory and Analytic Gradient Techniques. 1. *J. Phys. Chem. A* **1997**, *101*, 4263−4270.
(33) Yarkony, D. R. On the Construction of Diabatic Bases Using Molecular Properties. Rigorous Results in the Vicinity of a Conical Intersection. *J. Phys. Chem. A* **1998**, *102*, 8073−8077.
(34) Zhu, X.; Yarkony, D. R. Constructing Diabatic Representations Using Adiabatic and Approximate Diabatic Data − Coping with Diabolical Singularities. *J. Chem. Phys.* **2016**, *144*, 044104.
(35) Zhu, X.; Yarkony, D. R. On the Representation of Coupled Adiabatic Potential Energy Surfaces Using Quasi-Diabatic Hamiltonians: A Distributed Origins Expansion Approach. *J. Chem. Phys.* **2012**, *136*, 174110.

DOI: 10.1021/acs.jpca.9b08519
J. Phys. Chem. A 2019, 123, 9874−9880